



The mass accommodation coefficient of ammonium nitrate aerosol

Konstandinos G. Dassios, Spyros N. Pandis*

Departments of Chemical Engineering and Engineering and Public Policy, Carnegie Mellon University, Pittsburgh, PA 15213, USA

Received 1 August 1998; accepted 22 December 1998

Abstract

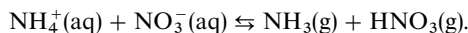
The mass transfer rate of pure ammonium nitrate between the aerosol and gas phases was quantified experimentally by the use of the tandem differential mobility analyzer/scanning mobility particle sizer (TDMA/SMPS) technique. Ammonium nitrate particles 80–220 nm in diameter evaporated in purified air in a laminar flow reactor under temperatures of 20–27°C and relative humidities in the vicinity of 10%. The evaporation rates were calculated by comparing the initial and final size distributions. A theoretical expression of the evaporation rate incorporating the Kelvin effect and the effect of relative humidity on the equilibrium constant is developed. The measurements were consistent with the theoretical predictions but there was evidence of a small kinetic resistance to the mass transfer rate. The discrepancy can be explained by a mass accommodation coefficient ranging from 0.8 to 0.5 as temperature increases from 20–27°C. The corresponding timescale of evaporation for submicron NH_4NO_3 particles in the atmosphere is of the order of a few seconds to 20 min. © 1999 Elsevier Science Ltd. All rights reserved.

Keywords: Ammonium nitrate; Evaporation; Accommodation coefficient; Kelvin effect; Inorganic aerosol

1. Introduction

Secondary inorganic aerosol (SIA) is formed in the atmosphere by homogeneous and heterogeneous reactions between gas-phase species. SIA consists mainly of ammonium, nitrate and sulfate and typically comprises 25–50% of the fine aerosol (Gray et al., 1986; Heintzenberg, 1989). Ammonium nitrate (NH_4NO_3) is a major component of SIA and is formed from the reaction between gas-phase ammonia – coming mainly from fertilizers, animals, and biological decay – and gas-phase nitric acid. Ammonium nitrate typically accounts for up to 10–30% of the fine aerosol mass (Wexler and Seinfeld, 1990), even more in some areas of the Western US and Northern Europe. A significant fraction of the aerosol NH_4NO_3 is associated with particles 100–300 nm in diameter (John et al., 1990). NH_4NO_3 is volatile under typical atmospheric conditions; it can evaporate

producing NH_3 and HNO_3 . The process is described by the reversible reactions



The direction of the reaction for pure ammonium nitrate particles depends on the ambient temperature and relative humidity. Those two factors determine the value of the equilibrium constant and drive the reaction to either the formation or evaporation of the particles. Ambient temperature and relative humidity values also specify the physical state of the NH_4NO_3 particles that can be either solid or liquid. NH_4NO_3 particles in typical ambient temperatures deliquesce at around 60% relative humidity but do not crystallize until relative humidity is decreased to less than 10% (Ten Brink, personal communication).

Several studies have theoretically described the NH_4NO_3 partitioning between gas and aerosol phases

*Corresponding author.

assuming thermodynamic equilibrium between the gas and particulate phases (Tanner, 1982; Bassett and Seinfeld, 1984; Hildemann et al., 1984; Chang et al., 1986; Walter et al., 1990; Bai et al., 1995). This assumption implies that the mass transfer rate is rapid enough compared to the timescale of interest so that the gas-phase concentrations of HNO_3 and NH_3 satisfy

$$c_{\text{NH}_3} \cdot c_{\text{HNO}_3} = K(T, \text{RH}),$$

where c_i are the concentrations of species $i = \text{NH}_3$, HNO_3 and $K(T, \text{RH})$ is the equilibrium constant for ammonium nitrate, calculated as a function of ambient temperature and relative humidity. This equation is applicable to pure ammonium nitrate particles. If sulfate or other electrolytes are present, K depends in general on their concentrations (Seinfeld and Pandis, 1998).

Field measurements of ammonia and nitric acid concentrations have in general supported the use of the equilibrium assumption (Spicer, 1974; Russell et al., 1983; Hildemann et al., 1984; Chang et al., 1986; Allen et al., 1989). However, the few available laboratory measurements of the NH_4NO_3 evaporation rate have yielded contradictory results. Most of these measurements suggest that the NH_4NO_3 evaporation rate is slower than mass transfer theory predictions (Larson and Taylor, 1983; Richardson and Hightower, 1987; Harrison et al., 1990). These discrepancies were reconciled by introducing the accommodation coefficient, α , a kinetics-originating factor describing the interface limitations to the mass transfer between the aerosol and gas-phases. The coefficient is yet not well understood; the process is believed to be inhibited by a resistance in transport of molecules across the particle/air interface. When α is unity there is no interfacial resistance. For fine particles that are in the kinetic and transition regimes, as α decreases surface accommodation starts limiting the overall transport rate (Seinfeld and Pandis, 1998). Our lack of understanding of the mass accommodation coefficient of semi-volatile aerosol species and especially ammonium nitrate is one of the most important obstacles in simulating their atmospheric concentrations (Wexler and Seinfeld, 1990).

Past experimental studies resulted in contradictory results regarding the value of the accommodation coefficient for ammonium nitrate. Larson and Taylor (1983), using aqueous NH_4NO_3 particles with a mass median diameter of 400 nm, reported an accommodation coefficient value of unity suggesting negligible resistance to mass transport of ammonium nitrate from the aerosol to the gas-phase. Richardson and Hightower (1987) measured changes in the size of NH_4NO_3 particles at low RH. They reported an evaporation rate 50 times lower than predicted and estimated accommodation coefficient values decreasing from 0.02 to 0.004 during the 4 h of their evaporation experiment. Harrison et al. (1990) measured the evaporation of NH_4NO_3 aerosol particles at

relative humidities of 97 and 30–60%, respectively. They reported that particles at low RH evaporate at a constant rate suggesting the probable existence of some kinetic constraint. Kirchner et al. (1990) used a technique involving a liquid jet technique to measure the absorption rates and, hence, mass accommodation coefficients of HCl, HNO_3 and N_2O_5 vapors on aqueous particles. The trace gases were introduced in a vertical flow tube with a known initial concentration where they are absorbed on the jet surface and diffused further into the liquid. The concentration of the trace gases after approximately 1 ms was measured to determine the extent of absorption and compare with theoretical predictions. They reported an accommodation coefficient greater than 0.01 for HNO_3 with their results showing negligible dependence on RH. Bergin et al. (1997) combined their light scattering coefficient measurements of ammonium nitrate aerosol with an evaporation model and reported an accommodation coefficient value close to unity. Their use of particles larger than 300 nm and the small evaporation of the particles resulted in significant uncertainty of the determined coefficient.

The above available information on NH_4NO_3 accommodation coefficient values is contradictory. At this time, aerosol models that require input of a value for this accommodation coefficient use values ranging from 0.001 to 1 (Wexler and Seinfeld, 1992; Meng and Seinfeld, 1995). A value of 0.01 was recently used in the Eulerian model of Meng et al. (1998). We need to decrease the uncertainty surrounding the NH_4NO_3 mass accommodation coefficient and its timescale of evaporation. Our approach will be to measure the size changes of evaporating ammonium nitrate particles at relative humidities as low as 10% where the particles are almost completely dehydrated. We use sensitive measurement techniques that enable us to examine particles in the lower end of the transition regime and compare the results with an updated theoretical model.

2. Theory

In this section, we derive an expression for the reduction in diameter of an ammonium nitrate particle evaporating in a constant temperature, relative humidity, and background $\text{HNO}_3(\text{g})$ and $\text{NH}_3(\text{g})$ concentrations environment. We assume that particles produced upon drying of droplets of ammonium nitrate solutions are spherical (Leong, 1981). An NH_4NO_3 particle introduced in a low NH_3/HNO_3 gaseous concentrations environment evaporates as the aerosol attempts to equilibrate with its surroundings. Neglecting latent heat effects and assuming dilute conditions, the diffusive molar flux in moles s^{-1} is (Seinfeld and Pandis, 1998):

$$J_{i,R_p} = -4\pi R_p D_{i,\text{air}} F(Kn_i, \alpha_i)(c_i^\infty - c_i), \quad (1)$$

where R_p is the particle radius, $D_{i,\text{air}}$ is the diffusivity of gas i ($i = \text{NH}_3, \text{HNO}_3$) in air, c_i^∞ and c_i are the concentrations of the species far from and at the particle surface, respectively, $Kn_i = \lambda_i/R_p$ is the Knudsen number and λ_i is the mean free path of gas i molecules. $F(Kn_i, \alpha_i)$ is the correction term for the kinetic and transition regime. Fuchs and Sutugin (1971) proposed the following expression

$$F(Kn_i) = \frac{1 + Kn_i}{1 + 0.3773Kn_i + 1.33Kn_i(1 + Kn_i)/\alpha_i}, \quad (2)$$

where α_i is the mass accommodation coefficient for gas i . For the purposes of this study we assume that $\alpha_{\text{NH}_3} = \alpha_{\text{HNO}_3} = \alpha_{\text{NH}_4\text{NO}_3} = \alpha$, effectively using the accommodation coefficient as a parameter to describe limitations to mass transfer.

A modified Kelvin equation can be used to account for the vapor pressure increase over the curved particle surface (Appendix A). The equilibrium condition, corrected to account for particle curvature, will then have the form

$$c_{\text{NH}_3}c_{\text{HNO}_3} = K(T, \text{RH})\exp\left(\frac{2\sigma v_l}{RTR_p}\right), \quad (3)$$

$$\frac{dD_p}{dt} = 2\frac{W}{W_0} \left[\beta - \sqrt{\gamma + 4D_{\text{HNO}_3}D_{\text{NH}_3}F(Kn_{\text{HNO}_3})F(Kn_{\text{NH}_3})K(T, \text{RH})\exp\left(\frac{2\sigma v_l}{RTR_p}\right)} \right] \text{MW}_{\text{NH}_4\text{NO}_3}, \quad (9)$$

where σ is the surface tension and v_l is the molecular volume of the particle.

At the particle surface, thermodynamic equilibrium is assumed to hold (Eq. (3)). The characteristic time to achieve equilibrium at the gas–particle interface is of the order of 10^{-5} s, four orders of magnitude less than the timescale of interest – a few seconds (Seinfeld and Pandis, 1998).

Stoichiometry indicates a 1 : 1 : 1 molar ratio of production of gaseous HNO_3 and NH_3 to consumption of NH_4NO_3 during evaporation, or

$$-J_{\text{NH}_3, \text{Rp}} = -J_{\text{HNO}_3, \text{Rp}} = J_{\text{NH}_4\text{NO}_3, \text{Rp}}, \quad (4)$$

where $J_{j, \text{Rp}}$ are the molar fluxes of $j = \text{NH}_3, \text{HNO}_3, \text{NH}_4\text{NO}_3$ at the particle surface.

Equating the two fluxes for the gaseous species as calculated from (1) and combining them with the equilibrium condition (3) one gets the transition-regime Kelvin-effect-corrected rate of evaporation of ammonium nitrate:

$$J_{\text{NH}_4\text{NO}_3, \text{Rp}} = 2\pi R_p \left[\beta - \sqrt{\gamma + 4D_{\text{HNO}_3}D_{\text{NH}_3}F(Kn_{\text{HNO}_3})F(Kn_{\text{NH}_3})K(T, \text{RH})\exp\left(\frac{2\sigma v_l}{RTR_p}\right)} \right] \quad (5)$$

where β and γ are given by

$$\beta = D_{\text{HNO}_3}c_{\text{HNO}_3}^\infty F(Kn_{\text{HNO}_3}) + D_{\text{NH}_3}c_{\text{NH}_3}^\infty F(Kn_{\text{NH}_3}), \quad (6)$$

$$\gamma = [D_{\text{HNO}_3}c_{\text{HNO}_3}^\infty F(Kn_{\text{HNO}_3}) - D_{\text{NH}_3}c_{\text{NH}_3}^\infty F(Kn_{\text{NH}_3})]^2, \quad (7)$$

and are zero in a purified air system. A similar expression without the Kelvin effect has been proposed by Wexler and Seinfeld (1990).

In order to convert the evaporation rate to a rate of change in size we use the mass balance for the particle

$$\frac{d}{dt} \left(\frac{4}{3}\pi R_p^3 \rho \right) = \frac{W}{W_0} J_{\text{NH}_4\text{NO}_3, \text{Rp}} \text{MW}_{\text{NH}_4\text{NO}_3}, \quad (8)$$

where $\text{MW}_{\text{NH}_4\text{NO}_3}$ is the molecular weight of ammonium nitrate, ρ is the particle density, W is the mass of the particle at the relative humidity of interest, and W_0 is the dry NH_4NO_3 particle mass. W/W_0 can be calculated using an atmospheric aerosol thermodynamics model (Ansari and Pandis, 1999) versus relative humidity. Finally, the rate of change in particle diameter due to evaporation is

Use of this expression requires the value of $K(T, \text{RH})$ which can also be estimated based on the model of Ansari and Pandis (1999).

2.1. Ammonium nitrate thermodynamics

Several expressions have been proposed for the dissociation constant of solid ammonium nitrate, $K(T)$, (Eq. (3)) and its dependence on temperature and relative humidity; the most frequently used ones are depicted in Fig. 1. The discrepancies suggest that theoretical models using different forms of $K(T)$ can lead to different estimates of the evaporation rate. The expression proposed by Mozurkewich (1993) will be used here because it reproduces better the available measurements of Tang et al. (1981) for the $(\text{NH}_4)_2\text{SO}_4\text{--NH}_4\text{NO}_3$ system (Ansari and Pandis, 1999), it uses updated thermodynamic data, and represents, in a sense, the average of the published equilibrium constants.

Recent experimental studies have shown that the crystallization RH of aqueous ammonium nitrate particles is

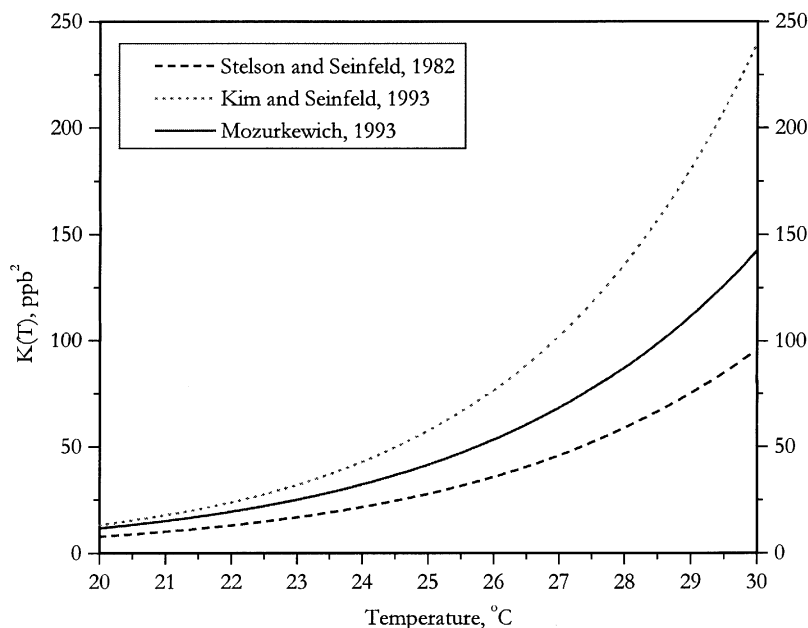


Fig. 1. Proposed forms of the dissociation constant of solid NH_4NO_3 as a function of temperature.

very low. It has been shown (Ten Brink, personal communication) that at relative humidity as low as 10%, NH_4NO_3 particles are still supersaturated aqueous solutions as a result of the hysteresis phenomenon. Models that describe the evaporation of particles that have been generated upon drying of an ammonium nitrate solution droplet should account for the presence of a supersaturated aqueous solution instead of a dry aerosol.

For a dry NH_4NO_3 particle, the dissociation constant remains the same for relative humidities less than the deliquescence relative humidity (approximately 60% for NH_4NO_3 at the temperature range of interest). However, for a supersaturated liquid NH_4NO_3 particle the gas-phase ammonia and nitric acid concentration product at the particle surface increases as relative humidity decreases below 60%. Fig. 2 shows the estimated dissociation constant for a wet NH_4NO_3 particle as a function of relative humidity at various temperatures using the Gibbs free energy minimization model (GFEMN) of Ansari and Pandis (1999). One should note the discrepancy between the values of the dissociation constant for the wet- and dry-particle cases. For example, at 40% RH and 25°C (Fig. 2), the “dry” and “wet” dissociation constant values differ by 45%. Thermodynamic data is available for the relative humidity range 40–94% and values below 40% are based on approximations for the dissociation constant.

3. Experimental

The technique used for measuring the change in size of the NH_4NO_3 particles is the tandem differential mobility

analyzer (TDMA) (Liu et al., 1977; Rader and McMurry, 1986). The experimental setup consists of two differential mobility analyzers (DMAs, TSI Inc., model no. 3071) working in series, an NH_4NO_3 particle generator and an evaporator (Fig. 3). Ammonia and nitric acid vapors are removed from the air stream using packed beds of citric acid and sodium bicarbonate. The NH_4NO_3 solution is initially atomized and a polydisperse water droplet distribution is generated. The particles are then dried in a silica gel dryer. The aerosol is next introduced into the first DMA (or DMA-1). A neutralizer applies an equilibrium bipolar charge on the particles and the DMA selects particles of a certain electrical mobility. Because the aerosols used in these experiments are smaller than 200 nm, practically all of the selected particles have a unit charge and thus have the same size. In that way DMA-1 transforms a polydisperse aerosol to a nearly monodisperse one with a known diameter.

The monodisperse aerosol is then introduced into a laminar flow reactor where particles are allowed to evaporate in an ammonia-, nitric acid-, organics-free environment at low relative humidity (around 10%). The 4-m long reactor (evaporator) consists of two concentric cylinders. A constant temperature bath is used to circulate water through the outer cylinder whereas the aerosol flows in the inner tube that is 2.54 cm in diameter. The aerosol stream is mixed with a purified airflow before entering the evaporator, heated to the same temperature as the outside water in order to provide isothermal conditions throughout the process. An average residence time of 30 s is used in most experiments. Downstream the evaporator particles from the centerline streamlines are

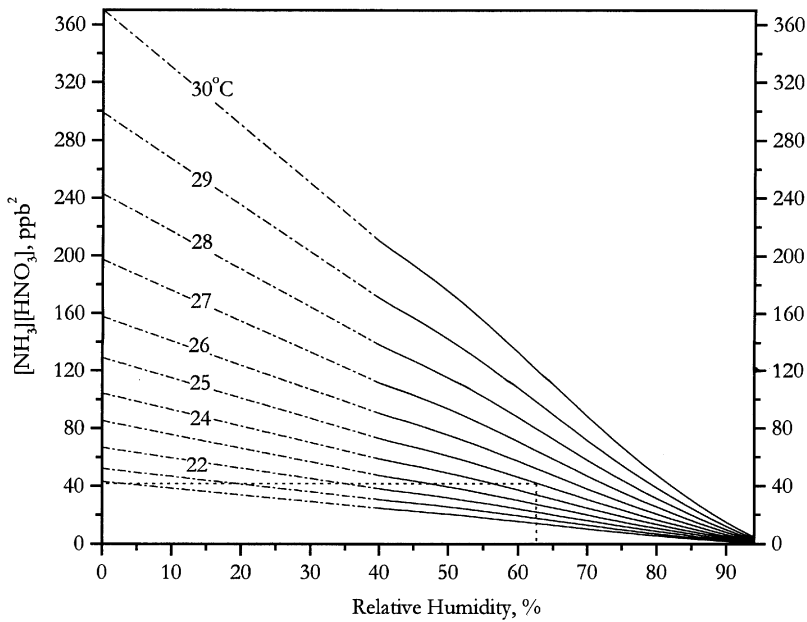


Fig. 2. Predicted equilibrium constant ($K = [\text{NH}_3(\text{g})][\text{HNO}_3(\text{g})]$) for aqueous NH_4NO_3 solutions as a function of RH and temperature. Solid lines are the results of the GFEMN model (Ansari and Pandis, 1999) whereas dashed lines are extrapolations for the low RH range. The dotted line represents $K(T)$ for a dry particle at 25°C below its DRH.

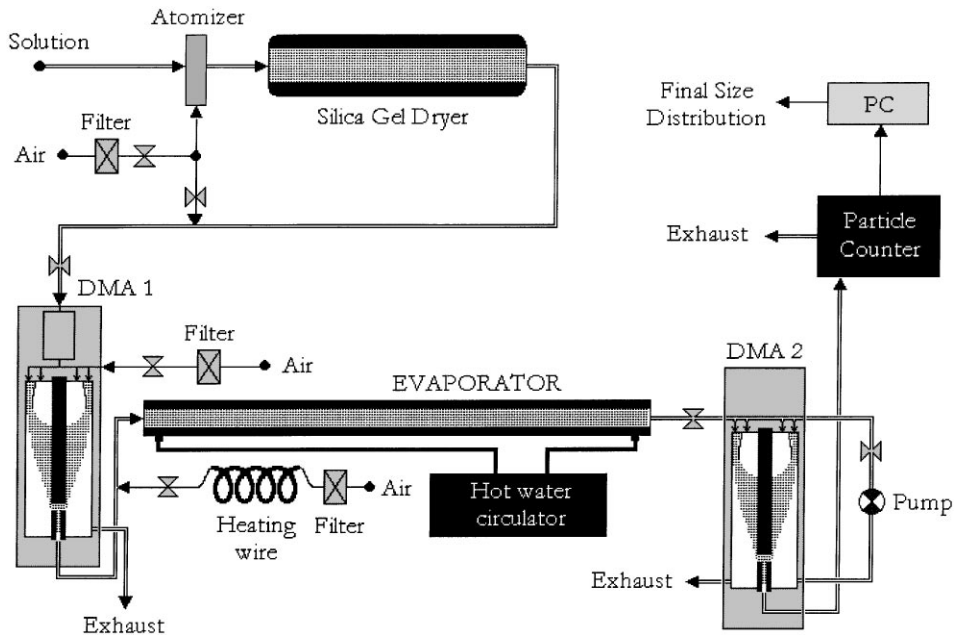


Fig. 3. TDMA/SMPS experimental setup. Laminar flow conditions apply throughout the process including inside the DMAs.

introduced in a scanning mobility particle sizer system (SMPS, TSI Model 3934) consisting of a second DMA (DMA-2) and a particle counter (Condensation Nuclei Counter, TSI Inc., Model 3010). DMA-2 scans the entire

voltage range and thus the final size distribution is measured.

Experiments were run for initial particle diameters in the range of 80–220 nm and for temperatures in the range

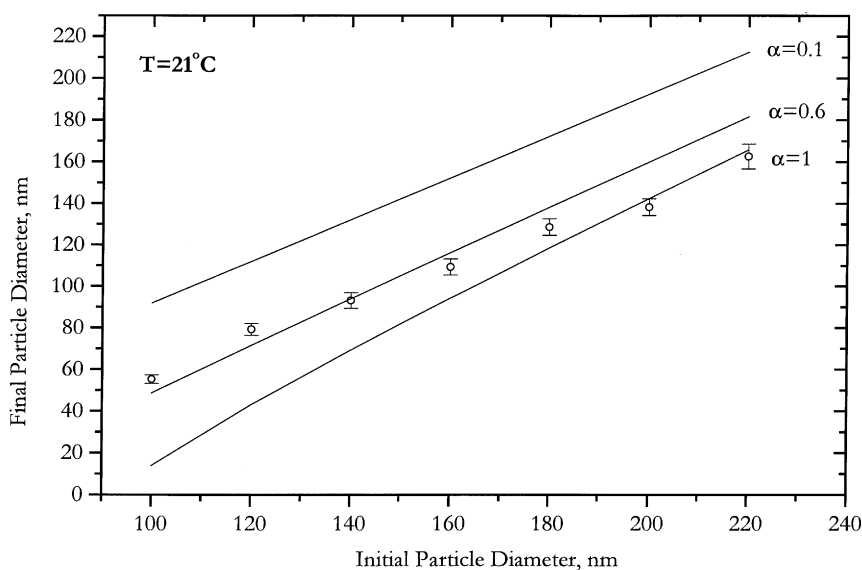


Fig. 4. Results from experiments run at 21°C. Circles represent the experimental measurements and error bars indicate one deviation from the mean diameter observed. The solid line represents theoretical predictions for different values of the accommodation coefficient.

of 20–27°C. To account for evaporation of the NH_4NO_3 inside the DMAs and connecting tubing and discrepancies between the two DMAs, calibration experiments were run without the evaporator. The reduction in diameter was found to be 2% or less. This change was then used to correct the initial diameter during the main experiments. The change in diameters reported in the following sections have been corrected, and therefore correspond to evaporation inside the laminar flow reactor only.

4. Results

Results of evaporation experiments run at 21°C are presented in Fig. 4. Relative humidity in the evaporator was measured to be around 10% for all experiments. At this relative humidity, particles are still wet and the corresponding values for the dissociation constant from Fig. 2 are used in the theoretical model. The measurements lie in the region defined by the two theoretical predictions for accommodation coefficient values of 1.0 and 0.6 (solid lines). The accommodation coefficient value that can best fit the results is around $\alpha = 0.8$. Also plotted is the $\alpha = 0.1$ case that is clearly over-predicting the observed final diameters at this temperature. Fig. 4 appears to indicate that the accommodation coefficient increases from 0.6 to 1.0 as the particle diameter increases from 100–220 nm. However, such a dependence of the accommodation coefficient on size for such particles is unreasonable. Uncertainties in the measurements, transition regime theory, and parameters used are probably the cause for this apparent change.

Results for experiments at four temperatures in the range 20–27°C are presented in Fig. 5. Theoretical predictions in Fig. 5 are obtained using the best-fit accommodation coefficient value for each temperature. These values were calculated in the same way as in the 21°C case discussed above. Results indicate the general consistency of the measurements with the mass transfer expression of Eq. (9) using $\alpha = 0.5$ –0.8. Evaporation is slower than what theory for $\alpha = 1$ predicts and a non-unity accommodation coefficient is necessary to describe the observed evaporation rate. The measured accommodation coefficient appears to decrease with temperature from 0.8 at 21°C to 0.5 at 27°C.

Fig. 6 depicts the $\alpha = 1$ case that frequently under-predicts the results, especially for the final particle diameters of less than 80 nm. These results illustrate the sensitivity of our measurements to the accommodation coefficient value used.

These results are in quantitative agreement with the suggestion of Clement et al. (1996), based on theoretical arguments, that general values of accommodation coefficients can differ somewhat from unity but they should not be much less than that in conditions and processes having atmospheric relevance.

4.1. Sensitivity analysis and discussion

A number of uncertain parameters are used in our theoretical model. These parameters could potentially explain the apparent deviation of the measurements from the theoretical ($\alpha = 1$) results. Their effects are discussed below.

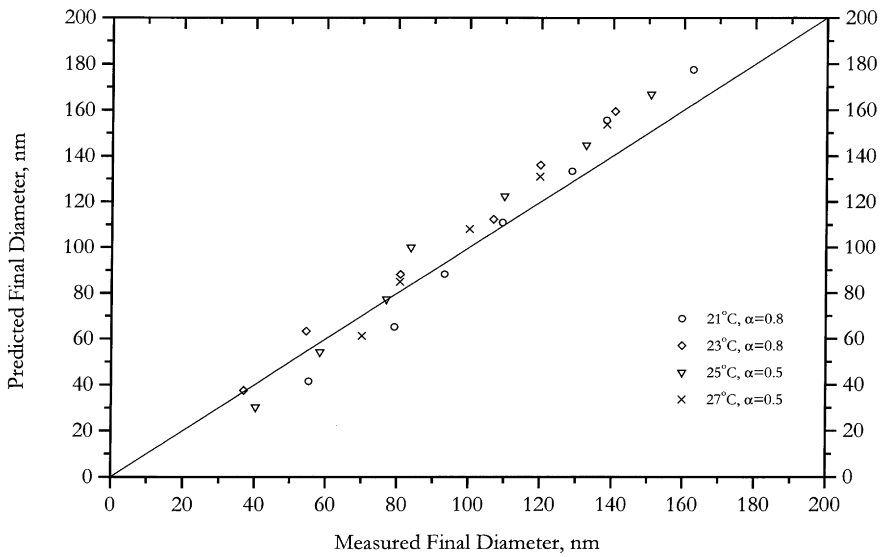


Fig. 5. Experimentally observed vs. theoretically predicted values of the final diameter for the best-fit value of accommodation coefficient.

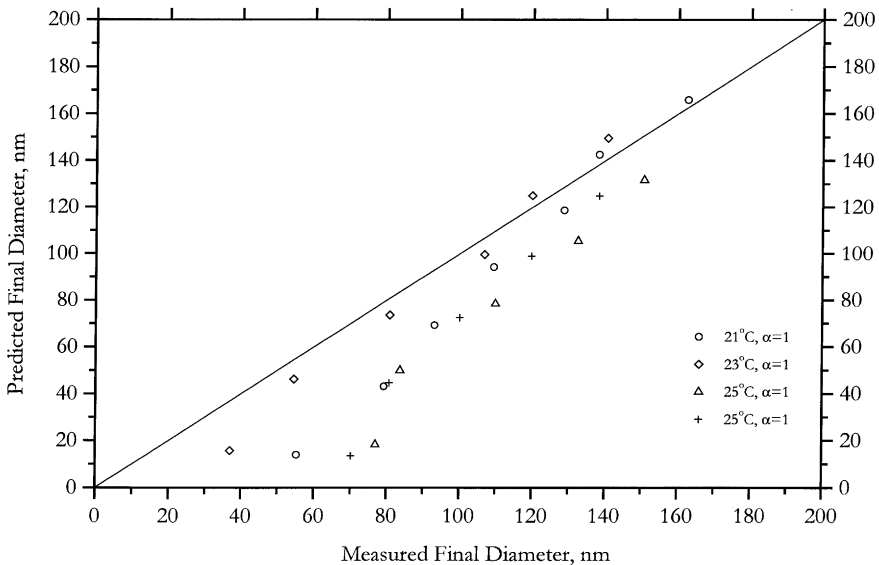


Fig. 6. Experimentally observed vs. theoretically predicted values of final diameter for the unity accommodation coefficient case.

The equilibrium constant is a strong function of temperature (Fig. 1). Any temperature gradient throughout the process would influence our results. We have been constantly measuring the temperature at five sampling points throughout the evaporator and deviations of a maximum of $\pm 0.1^\circ\text{C}$ were observed, proving the validity of isothermal conditions. We estimated that a reduction in $K(T, \text{RH})$ by as much as a factor of four is necessary to explain the lower evaporation rates. For

example, at 25°C , the wet-particle dissociation constant used in the model is approximately 130 ppb^2 and the value that would match the results to the theory for a unity accommodation coefficient is 25 ppb^2 . This relatively small sensitivity to $K(T, \text{RH})$, is the result of the square root dependence of the evaporation rate on $K(T, \text{RH})$ (Eqs. (5) and (9)). An error of approximately 2.5°C is necessary and this possibility can therefore be excluded. The dependence of the equilibrium constant on

Table 1
Model sensitivity for the evaporation of a 160 nm particle at 23°C

Parameter	Value used	Perturbed by	Effect on final diameter (nm)
Surface tension, (ergs cm ⁻²)	120	+ 10% - 50%	- 0.4 + 2.2
Diffusivity, (cm ² s ⁻¹)	0.11	+ 10% - 10%	- 3 + 3.7
W/W_0	1.05 (at 10%RH)	+ 25%	- 2

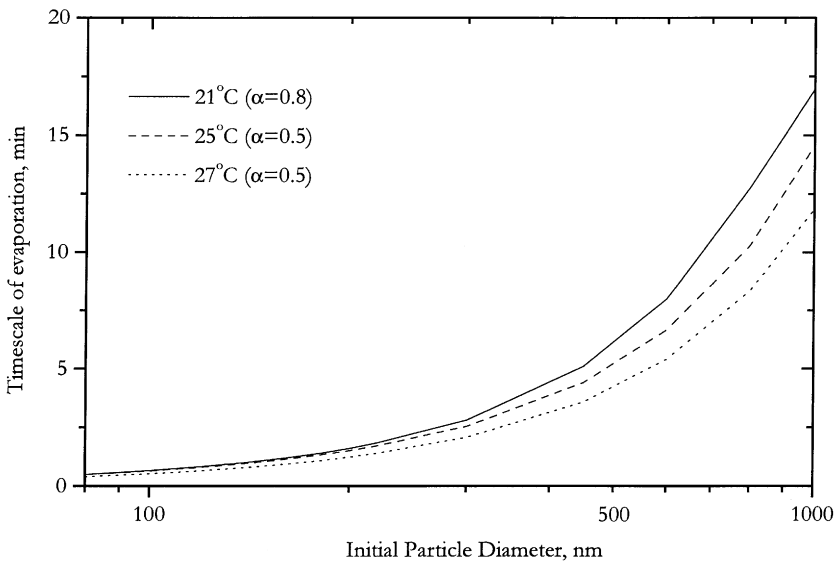


Fig. 7. Estimated characteristic times for mass transfer of ammonium nitrate aerosol between the aerosol and gas phase for ambient temperatures of 21, 25 and 27°C.

RH is also uncertain, especially for this low RH region (Fig. 2). However, the observations once more cannot be explained by either small errors in RH or by the uncertainty of the constant dependence on RH.

Non-zero gaseous concentrations of ammonia and nitric acid can bring the system closer to equilibrium and explain a slower evaporation rate. To verify the efficient removal of these species, we run additional experiments with double pairs of air purifying filters working in series and we obtained the same results. Also, a mass balance on the NH₃ and HNO₃ vapor accumulation during evaporation showed their concentrations to be negligible. The estimated concentration of the vapors produced from the evaporation of NH₄NO₃ are not sufficient to slow down the rate of evaporation by more than a few percent. Our results were also invariant to the number of particles present proving that the gas-phase concentrations of NH₃ and HNO₃ produced during evapor-

ation have negligible influence on the evaporation rate.

A sensitivity analysis of the model to parameters such as the surface tension and the diffusivity is presented in Table 1 for a 160 nm particle and a temperature of 23°C. Using a surface tension value even lower than that of pure water fails to reproduce the final diameter observed. A W/W_0 value corresponding to 50% RH still only slightly affects the final diameter. The effect of these parameters on the final diameter is minor and cannot explain the deviations of measurements from the $\alpha = 1$ theoretical predictions.

For the case where particles are solid, the dissociation constant for all temperatures is significantly less than the case we are examining, as previously discussed in the thermodynamics section. The corresponding theoretical driving force for evaporation is then too small and cannot explain the observed evaporation rate. Only

an accommodation coefficient greater than unity can match the measurements to theory in this case. This provides indirect evidence that our particles were indeed wet.

4.2. Timescale of evaporation

The characteristic time for the aerosol-to-gas phase transport is of particular importance for understanding the behavior of ammonium nitrate in our atmosphere. The timescale of evaporation of an ammonium nitrate particle of initial diameter R_p can be computed using the theoretical model with the measured values of the accommodation coefficient at each temperature. This timescale varies from a fraction of a second to several minutes, as shown in Fig. 7. These values are in the low range of the evaporation timescales calculated by Wexler and Seinfeld (1992). Along with the accommodation coefficient values, these calculated timescales can be used in current aerosol models to help better describe the dynamic transport of ammonium nitrate between the gas and aerosol phases (Meng and Seinfeld, 1995; Pandis et al., 1995). Aerosol associated with the submicron size range can be considered to be in equilibrium with the gas-phase species since the equilibration time of a few minutes is small compared to other relevant timescales. For particles larger than $1\ \mu\text{m}$ the timescale for equilibration is of the order of an hour or more. For example, for a particle with a diameter equal to $5\ \mu\text{m}$ at 298 K, an equilibration timescale of roughly 5 h is estimated. The assumption of thermodynamic equilibrium will not be applicable in general for the coarse-mode nitrate (Meng and Seinfeld, 1995). The calculated timescale is sensitive to changes in temperature but not to relative humidity or gas-phase concentrations.

5. Conclusions

We used the TDMA/SMPS system to measure the change in diameter of ammonium nitrate aerosol that evaporated for approximately 30 s in a pure-air environment at low RH. Relative humidity was measured to be around 10%, and experiments were run for temperature values in the range of 20–27°C. The system showed a dynamic behavior slightly slower than traditional non-continuum regime mass transfer theory predictions. The process of evaporation of ammonium nitrate aerosol particles can be described by using a temperature-dependent accommodation coefficient varying from 0.8 to 0.5 in the temperature range of 20–27°C.

The timescale for mass transfer and equilibration of ammonium nitrate associated with the sub-micron ambient aerosol is estimated to be a few minutes. Particles smaller than 100 nm in diameter can equilibrate in a few seconds under typical temperatures. These results suggest

that submicron particles can be considered to be in equilibrium with their gaseous precursors as the correspondent timescale is very short compared to other atmospheric timescales of interest.

Our study focused on pure ammonium nitrate particles and did not consider other resistances to mass transfer (organic films, “trapping” of NH_4NO_3 inside the particles, etc.) that could potentially slow down the NH_4NO_3 mass transfer in the ambient atmosphere. These potential resistances will be the focus of additional studies.

Acknowledgements

We thank M. Bergin for his comments, A. Khlystov and T.M. Ten Brink for sharing their experimental data and Asif Ansari for his help with the thermodynamic calculations. This research was supported by the US Environmental Protection Agency (R-823514).

Appendix A

Kelvin effect

The change of Gibbs free energy accompanying the formation of a single particle of pure ammonium nitrate containing n molecules of the substance is

$$\Delta G = n(g_s - g_{v1} - g_{v2}) + 4\pi R_p^2 \sigma, \quad (10)$$

where g_s is the Gibbs free energy of a NH_4NO_3 molecule in the solid phase, g_{v1} and g_{v2} are the Gibbs free energies of HNO_3 and NH_3 molecules in the vapor phase and the last term is the free energy associated with radius of curvature R_p and surface tension σ .

The number of molecules in the particle, n , and the drop radius are related by

$$n = \frac{4\pi R_p^3}{3v_l}, \quad (11)$$

where v_l is the volume occupied by a molecule in the solid phase. The change in Gibbs free energy, g , for a constant-composition solid phase and isothermal conditions is

$$dG = -\frac{kT}{p} dp, \quad (12)$$

k , p , T denoting the Boltzmann constant, pressure and temperature, respectively. By integration of (12) we get

$$g_s - g_{v1} - g_{v2} = -kT \ln \frac{p_1^{\text{curved}}}{p_1^{\text{flat}}} - kT \ln \frac{p_2^{\text{curved}}}{p_2^{\text{flat}}}, \quad (13)$$

where p_i^{flat} is the vapor pressure of gas i over a flat surface and p_i^{curved} is the actual equilibrium partial pressure over the solid. Combining (10), (11) and (13) we get

$$\Delta G = -\frac{4\pi R_p^3}{3\nu_l} kT \ln \frac{p_1^{\text{curved}} p_2^{\text{curved}}}{p_1^{\text{flat}} p_2^{\text{flat}}} + 4\pi R_p^2 \sigma, \quad (14)$$

ΔG is minimum at the point where

$$\frac{\partial \Delta G}{\partial R_p} = 0 \quad (15)$$

or at

$$R_p^* = \frac{2\sigma\nu_l}{kT \ln \frac{(p_1^{\text{curved}} p_2^{\text{curved}})}{(p_1^{\text{flat}} p_2^{\text{flat}})}}. \quad (16)$$

Rearranging, the Kelvin equation for ammonium nitrate is

$$c_{\text{HNO}_3}^{\text{curv}} c_{\text{NH}_3}^{\text{curv}} = c_{\text{HNO}_3}^{\text{flat}} c_{\text{NH}_3}^{\text{flat}} \exp\left(\frac{2\sigma\nu_l}{RT R_p}\right). \quad (17)$$

References

- Allen, A.G., Harrison, R.M., Erisman, J.-W., 1989. Field measurements of the dissociation of ammonium nitrate and ammonium chloride aerosols. *Atmospheric Environment* 23, 1591–1599.
- Ansari, A.S., Pandis, S.N., 1999. Prediction of multicomponent inorganic atmospheric aerosol behavior. *Atmospheric Environment*, 33, 745–757.
- Bai, H., Lu, C., Ling, Y.M., 1995. A theoretical study on the evaporation of dry ammonium chloride and ammonium nitrate aerosols. *Atmospheric Environment* 29, 313–321.
- Bassett, M.E., Seinfeld, J.H., 1984. Atmospheric equilibrium model of sulfate and nitrate aerosols. *Atmospheric Environment* 17, 2237–2252.
- Bergin, M.H., Orgen, J.A., Schwartz, S.E., McInnes, L.M., 1997. Evaporation of ammonium nitrate aerosol in a heated nephelometer: implications for field measurements. *Environmental Science and Technology* 31, 2878–2883.
- Chang, Y.S., Carmichael, G.R., Kurita, H., Ueda, H., 1986. An investigation of the formation of ambient NH_4NO_3 aerosol. *Atmospheric Environment* 20, 1969–1977.
- Clement, C.F., Kulmala, M., Vesala, T., 1996. Theoretical consideration of sticking probabilities. *Journal of Aerosol Science* 27, 869–882.
- Fuchs, N.A., Sutugin, A.G., 1971. High dispersed aerosols, in *Topics in Current Aerosol Research (Part 2)*. Pergamon Press, New York.
- Gray, H.A., Cass, G.R., Huntzicker, J.J., Heyerdahl, E.K., Rau, J.A., 1986. Characteristics of atmospheric organic and elemental carbon particle concentrations in Los Angeles. *Environmental Science and Technology* 20, 580–589.
- Harrison, R.M., Sturges, W.T., Kitto, A.-M.N., Li, Y., 1990. Kinetics of evaporation of ammonium chloride and ammonium nitrate aerosols. *Atmospheric Environment* 24A, 1883–1888.
- Heintzenberg, J., 1989. Fine particles in the global troposphere. A review. *Tellus* 41B, 149–160.
- Hildemann, L.M., Russell, A.G., Cass, G.R., 1984. Ammonia and nitric acid concentrations in equilibrium with atmospheric aerosols: experiment vs theory. *Atmospheric Environment* 18, 1737–1750.
- John, W., Wall, S.M., Ondo, J.L., Winklmayr, W., 1990. Modes in the size distributions of atmospheric inorganic aerosol. *Atmospheric Environment* 24A, 2349–2359.
- Kirchner, W., Welter, F., Bongartz, A., Kames, J., Schweighoefer, S., Schurath, U., 1990. Trace gas exchange at the air/water interface: measurements of mass accommodation coefficients. *Journal of Atmospheric Chemistry* 10, 427–429.
- Larson, T.V., Taylor, G.S., 1983. On the evaporation of ammonium nitrate aerosol. *Atmospheric Environment* 17, 2605–2610.
- Leong, K.H., 1981. Morphology of aerosol particles generated from the evaporation of solution drops. *Journal of Aerosol Science* 12, 417–435.
- Liu, B.Y.H., Pui, D.Y.H., Whitby, K.T., Kittelson, D.B., Kousaka, Y., McKenzie, R.L., 1977. The aerosol mobility chromatograph: A new detector for sulfuric acid aerosols. *Atmospheric Environment* 12, 99–104.
- Meng, Z., Dabdub, D., Seinfeld, J.H., 1998. Size-resolved and chemically resolved model of atmospheric aerosol dynamics. *Journal of Geophysical Research* 103, 3419–3435.
- Meng, Z., Seinfeld, J.H., 1995. Timescales to achieve atmospheric gas-aerosol equilibrium for volatile species. *Atmospheric Environment* 16, 2889–2900.
- Mozurkewich, M., 1993. The dissociation constant of ammonium nitrate and its dependence on temperature, relative humidity and particle size. *Atmospheric Environment* 27A, 261–270.
- Rader, D.J., McMurry, P.H., 1986. Application of the Tandem Differential Mobility analyzer to studies of droplet growth or evaporation. *Journal of Aerosol Science* 17, 771–787.
- Richardson, C.B., Hightower, R.L., 1987. Evaporation of ammonium nitrate particles. *Atmospheric Environment* 21, 971–975.
- Russell, A.G., McRae, G.J., Cass, G.R., 1983. Mathematical modeling of the formation and transport of ammonium nitrate aerosol. *Atmospheric Environment* 17, 949–964.
- Pandis, S.N., Wexler, A.S., Seinfeld, J.H., 1995. Dynamics of tropospheric aerosols. *Journal of Physical Chemistry* 99, 9646–9659.
- Seinfeld, J.H., Pandis, S.N., 1998. *Atmospheric Chemistry: Air Pollution to Global Change*. Wiley, New York.
- Spicer, C.W., 1974. The fate of nitrogen oxides in the atmosphere. *Battelle Columbus Report To Coordinating Res. Council and US Environ. Protection Agency Report* 600/3-76-030.
- Tang, I.N., Wong, W.T., Munkelwitz, H.R., 1981. The relative importance of atmospheric sulfates and nitrates in visibility reduction. *Atmospheric Environment* 12, 2463–2471.

- Tanner, R.L., 1982. An ambient experimental study of phase equilibrium in the atmospheric system: aerosol H^+ , NH_4^+ , SO_4^{2-} , NO_3 , $\text{NH}_3(\text{g})$, $\text{HNO}_3(\text{g})$. *Atmospheric Environment* 16, 2935–2942.
- Walter, J., Wall, S.M., Ondo, J.L., Winklmayr, W., 1990. Modes in the size distributions of atmospheric inorganic aerosol. *Atmospheric Environment* 24A, 2349–2359.
- Wexler, A.S., Seinfeld, J.H., 1990. The distribution of ammonium salts among a size and composition dispersed aerosol. *Atmospheric Environment* 24A, 12 331–12 346.
- Wexler, A.S., Seinfeld, J.H., 1992. Analysis of aerosol equilibrium ammonium nitrate: departures from equilibrium during SCAQS. *Atmospheric Environment* 26A, 579–591.